

# DESIGN AND INTEGRATION OF MZI MODULATORS AND AWG-BASED MULTIWAVELENGTH LASERS IN InP

W. Pascher<sup>1</sup>, J.H. den Besten<sup>2</sup>, D. Caprioli<sup>2</sup>, R. van Dijk<sup>3</sup>, F.E. van Vliet<sup>3</sup>,  
J.J.M. Binsma<sup>4</sup>, E. Smalbrugge<sup>2</sup>, T. de Vries<sup>2</sup>, R.G. Broeke<sup>2</sup>,  
Y.S. Oei<sup>2</sup>, E.A.J.M. Bente<sup>2</sup>, X.J.M. Leijtens<sup>2</sup> and M.K. Smit<sup>2</sup>

<sup>1</sup> *Electromagnetic Field Theory, University Hagen, Hagen, Germany*

*W.Pascher@Fernuni-Hagen.de*

<sup>2</sup> *COBRA Research Institute, Technische Universiteit Eindhoven, Eindhoven, The Netherlands*

<sup>3</sup> *TNO Physics and Electronics Laboratory, The Hague, The Netherlands*

<sup>4</sup> *Formerly with JDS Uniphase, Eindhoven, The Netherlands.*

## ABSTRACT

The first Mach-Zehnder interferometer (MZI) modulator integrated with an arrayed-waveguide grating (AWG) based laser shall be demonstrated. A novel 4-channel device as small as  $4 \times 8 \text{ mm}^2$  is realized, employing only one AWG instead of three needed conventionally. Integration of two required epitaxial layerstacks was realized by growing one waveguide layer, locally removing it and regrowing a second layer in the etched region. The modulator design is optimized using rigorous field simulation of the complex semiconductor layer stack. Almost perfect velocity match and low microwave loss are obtained by  $1 \mu\text{m}$ -narrow waveguides with a  $2 \mu\text{m}$  signal electrode on top.

## INTRODUCTION

Dense integration of lasers with other components is a hot research topic since the laser output serves as an optical carrier for on-chip processes such as light conversion or modulation. Examples of advanced photonic integrated circuits (PICs) are a distributed feed-back laser (DFB) with an electro-absorption modulator (EAM) [1], a distributed Bragg reflector (DBR) laser with a Mach-Zehnder interferometer (MZI) modulator [2], and an arrayed-waveguide grating (AWG) based laser (AWGL) with a wavelength converter [3].

Our goal has been to demonstrate the first MZI modulator integrated with an AWGL (total device size:  $4 \times 8 \text{ mm}^2$ ). An AWGL has the advantage over a DBR or DFB laser that it can not only be utilized as a widely-tunable laser, but also as a multiwavelength source that generates multiple wavelengths simultaneously. This enables the integration of multiple modulators with only one AWGL to create an emitter of several wavelengths that can be modulated independently. — For integrating of both an active ( $\lambda_g = 1550 \text{ nm}$ ) and passive ( $\lambda_g = 1250 \text{ nm}$ ) film layer in the AWG-based Fabry-Pérot laser, we applied a three-step MOVPE butt-joint coupling technique. This also enables a doping profile in the passive sections that is optimal for the electro-optical phase-shifting Mach-Zehnder arms. Furthermore, since the Mach-Zehnder modulators require a layerstack with a semi-insulating substrate, the semiconductor optical amplifiers (SOAs) in the laser are equipped with a lateral n-contact instead of a conventional bottom contact.

The design of an MZI modulator is governed by two key properties: good velocity match between optical wave and microwave as well as low microwave loss. Hence a highly accurate model for microwave and optical propagation in an electro-optic modulator is needed that includes the loss in the modulating electrodes and in the inhomogeneous semiconductor layer stack. For this purpose the method of lines (MoL) is employed, a full wave simulation tool especially suited for complicated layer stacks [4]. In order to have a high modulation efficiency as well as a low microwave attenuation, the p-doped waveguide cladding should be as narrow and highly doped as possible. For this reason, the modulators are realized as  $1 \mu\text{m}$ -narrow deeply etched waveguides with a  $2 \mu\text{m}$  signal electrode on top. This reduces the microwave index and we obtain an almost perfect velocity match with the optical wave. Moreover, the impedance of the modulator increases and excellently matches with the driver.

This paper describes the development and realization of a novel 4-channel AWGL with four MZI modulators, four SOAs (one for each wavelength) and only one AWG. A conventional approach would need three AWGs: one in the multiwavelength laser and two at both ends of the modulators, for demultiplexing and multiplexing the wavelengths before and after modulation, respectively. This introduces complications: a large chip space is needed and all (de)multiplexers should be accurately tuned to each other. Our new approach performs all required multiplexing and demultiplexing operations with a single AWG. We hope to present first measurement results at the conference.

---

<sup>2</sup>This work was carried out under the framework of the European OBANET IST-2000-25390 project and the Dutch NRC-Photonics programme.

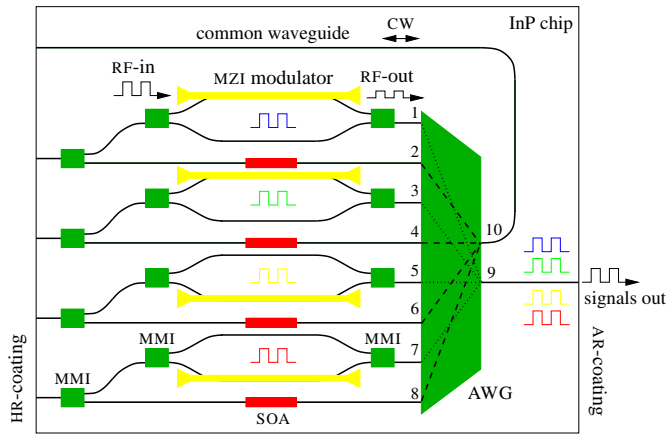


Fig. 1. Schematic of the 4- $\lambda$  multiwavelength laser integrated with only one AWG and four modulators.

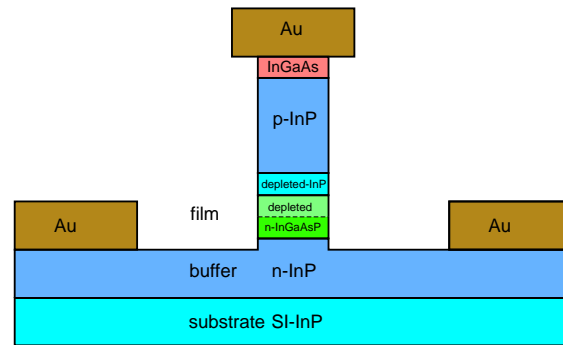


Fig. 2. Cross-section of the layer stack of a deeply etched MZI modulator with a 1  $\mu\text{m}$ -narrow waveguide.

## DESIGN AND MODELLING

To explain the operating principle of this device, we labelled all AWG ports in Fig. 1. At the right side of the AWG, the port with label 9 is the common output for fiber coupling and the port with label 10 is the common output that leads to a HR coated facet. This waveguide is part of the laser cavity. At left side of the AWG the demultiplexed ports are labelled 1 to 8. The even port-numbers (2, 4, 6 and 8) are each part of a different laser cavity (one for each wavelength) and are connected to 2- $\mu\text{m}$ -wide, 1000- $\mu\text{m}$ -long SOAs. From there, the cavities are completed by waveguides that lead to the HR coated facet.

In each cavity, a  $1 \times 2$  MMI is included to couple out half of the light reflected from the facet. This light is routed to a separate MZI modulator. They each modulate the microwave signals onto the optical carrier coming from the laser cavities. The four modulated signals at the uneven port-numbers (1, 3, 5 and 7) are multiplexed by the AWG to output port 9. The PICs have been fabricated in two successive fabrication runs, in which a number of technological problems have been identified and solved.

The microwave and optical properties of an electro-optic modulator are rigorously modeled including the loss in the modulating electrodes and in the inhomogeneous semiconductor layer stack. The model structure is analyzed by the method of lines (MoL), a finite difference approach, which has been efficiently used for the simulation of various planar waveguides in both integrated optics and microwave circuits. The planar layer stack is discretized in horizontal direction, whereas the wave equation is solved analytically in the vertical direction. Using the MoL we achieve very accurate results,

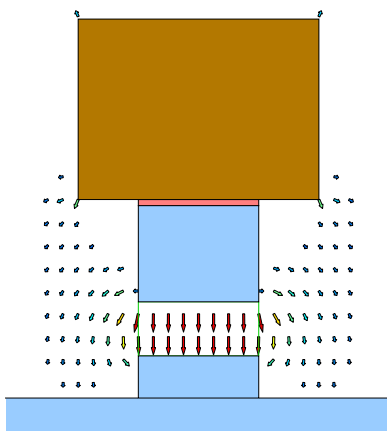


Fig. 3. Microwave electric field in the cross-section of the optimized modulator (arrow length proportional to field, only arrows above 25% of maximum field shown).

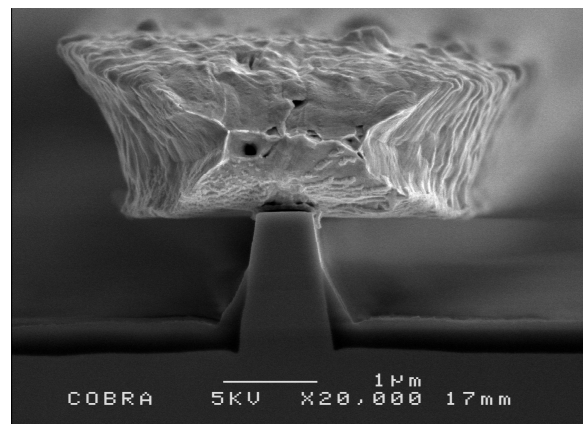


Fig. 4. Scanning Electron Microscope cross-section photograph with signal electrode on top of a 1- $\mu\text{m}$ -wide optical waveguide.

especially in the design curves for minimum microwave loss and in the electric field in the modulator.

Fig. 2. shows the cross-section of the investigated InP-based Mach-Zehnder modulator. The RF-signal is fed to one of the interferometer arms by a coplanar waveguide (CPW). There, the CPW is transferred into a microstrip by a  $N^+$ -buffer layer underneath an optical ridge waveguide. Its film layer consists of 500-nm-thick InGaAsP with a bandgap wavelength of  $1.25 \mu\text{m}$  (Q1.25). The InP-cladding is built up by a 200-nm-thick intrinsic layer and a p-doped layer. This layerstack configuration is similar to the passive waveguide structure used in the tunable laser integrated with a wavelength converter published by Broeke et al. [3], indicating the high integration potential of the device discussed here.

To have a high modulation efficiency and a low microwave attenuation at the same time, the p-doped cladding should be as narrow and highly doped as possible. With respect to the modulator investigated in [4], we changed the phase shifters from a  $4 \mu\text{m}$ -wide shallowly etched waveguide into a  $1 \mu\text{m}$ -wide deeply etched waveguide. This causes a reduction of the microwave index and a slight increase in the optical group index. An almost perfect velocity match is achieved.

The microwave electrical field distribution for the optimized design, namely in the region of the signal electrode is presented in Fig. 3. Due to the pin-structure of the optical waveguide, the microwave field is mainly across the depleted region, which consists of the upper part of the film layer and the intrinsic layer. The mode observed is nearly a microstrip mode because of the comparatively high conductivity of the n-doped buffer layer, which behaves like a ground plane.

## TECHNOLOGY AND CHARACTERIZATION

The integration of passive waveguides, optical amplifiers and RF phase shifters for use in a laser-modulator device requires optimization of the following issues: optical propagation, optical reflections, microwave coplanar waveguide (CPW) feed-line propagation, microwave phase-shifter propagation and SOA contacts. For the amplifiers, we developed a lateral n-metallization since the semi-insulating substrate does not allow for back-side metallization. For the waveguide etch, we applied both a Ti-mask and a  $\text{SiN}_x$ -mask to obtain different etch depths. This resulted in a  $1\text{-}\mu\text{m}$ -wide deep waveguide (s. Fig. 4) with an attenuation of  $11 \text{ dB/cm}$  and a  $4\text{-}\mu\text{m}$ -wide shallow waveguide with an attenuation of  $1.5 \text{ dB/cm}$ . The signal width was increased from the target value due to over-exposure of the metalization resist. In order to investigate the optical propagation through passive waveguides, we cleaved off, and separately measured, the AWG of the device with four modulators. This AWG was chirped [5] to ensure lasing in a predefined AWG order. Fig. 5 (left) shows the measured AWG transmission curves.

Any microwave attenuation in the CPW feed lines will decrease the measured bandwidth of the modulator. This is because the higher frequencies will be more attenuated by the CPW feed line than the lower frequencies. Any attenuation in the CPWs from the phase shifters to the loads does not affect the modulation bandwidth as the microwave signal has already been modulated onto the optical carrier. We succeeded in fabricating low-loss CPWs using electro-plating of gold. Fig. 5 (right) shows the measured  $S$ -parameters of a  $1.4\text{-mm}$ -long CPW with a signal width of  $6.8 \mu\text{m}$ , a gap of  $5.6 \mu\text{m}$  and a ground line width of  $50 \mu\text{m}$ . From the low reflection ( $S_{11}, S_{22} < -18 \text{ dB}$ ), it can be concluded that the impedance of the lines is close the  $50 \Omega$  impedance of the network analyzer. The extracted impedance value at  $40 \text{ GHz}$  is  $53 \pm 2 \Omega$ . The transmission values ( $S_{12}, S_{21}$ ) have dropped by only  $1 \text{ dB}$  at  $40 \text{ GHz}$  compared to the low frequency value.

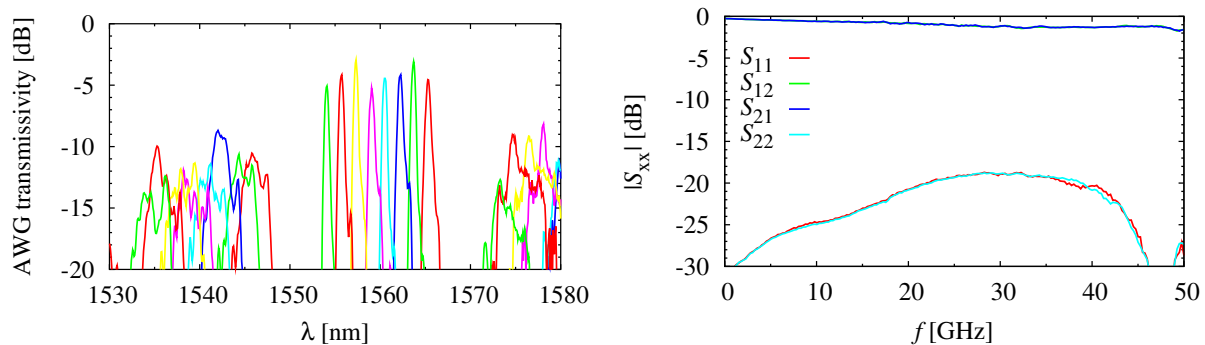


Figure 5: Measured chirped AWG passbands (left) and measured small-signal  $S$ -parameters of a CPW feed line with a length of  $1.4 \text{ mm}$  (right).

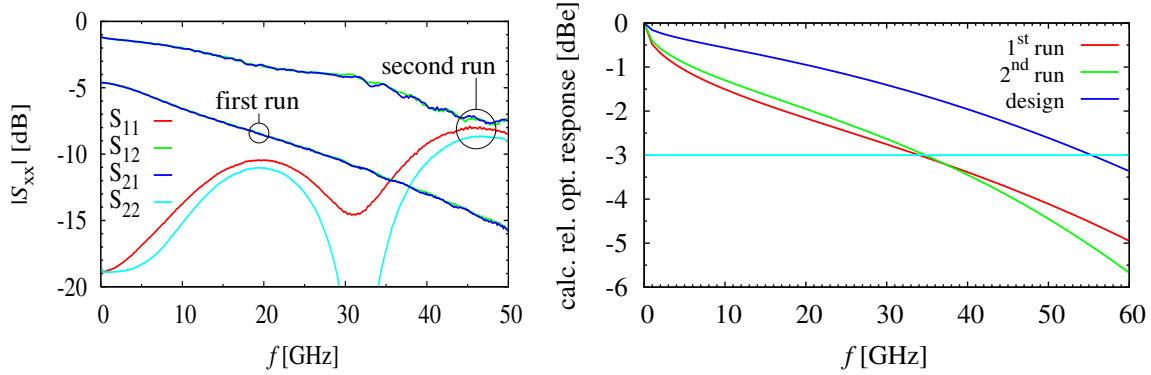


Figure 6: Measured  $S$ -parameters of a modulator with a phase-shifter length of 2 mm (*left*) and calculated bandwidth extracted from  $S$ -parameters measurements (*right*).

The microwave propagation in a phase shifter is characterized by two parameters: velocity and attenuation. The quality of the gold electrode on top of the MZI arm is of great influence on the microwave attenuation. The difference between the poor gold quality we had in the first fabrication run and the good quality of the second fabrication run is reflected in the small-signal  $S$ -parameter measurements on the modulator. In Fig. 6, a comparison is made between 2-mm-long phase shifters made in the first and second fabrication run, measured at a reverse bias of 5 V.

Several observations can be made. Firstly, for the second run, the  $S_{12}$  and  $S_{21}$  parameters start at a lower DC attenuation ( $\sim 1$  dB) than for the first run ( $\sim 4.5$  dB). This confirms that the gold quality has improved. Also the lower DC resistance confirmed an improvement of the gold quality. Phase shifters of 2 mm in length now had a resistance of  $17.98 \pm 4.15 \Omega$ . This is more than a factor two lower than for the first fabrication run. Secondly, the increase of the attenuation as a function of the frequency is less rapid: in the first run, the  $S_{12}$  and  $S_{21}$  parameters have dropped by 11 dB at 50 GHz, whereas this drop was only 7 dB at 50 GHz in the second run. From these measurements, we extracted the modulator impedance ( $49 \pm 3 \Omega$ ) and calculated the modulator bandwidth (Fig. 6 (*right*)). The expected bandwidth of the designed modulator is more than 55 GHz. The extracted bandwidth of the modulator of the first fabrication run was 34 GHz. The difference was only caused by the higher microwave attenuation in the gold, since the velocity match of this device was almost perfect. The modulator of the second fabrication run had a lower microwave attenuation than that of the first run, but experienced a slight velocity mismatch. This resulted in a similar bandwidth value (34 GHz), which is sufficient for 40 Gb/s operation.

## CONCLUSIONS

An ingenious multiwavelength laser layout as small as  $4 \times 8 \text{ mm}^2$  has been presented using four MZI modulators and only one AWG, which multiplexes all four signals into one output port thereby easing fiber-chip coupling. Excellent velocity match, low microwave loss and good impedance match are the features of the MZI modulator with a  $1 \mu\text{m}$ -narrow waveguide, which has been designed using a rigorous modeling by the vectorial Method of Lines (MoL). The fabrication of the PIC is challenging and several aspects have been discussed here. The achievements are an important step in the field of dense active-passive integration of PICs.

## REFERENCES

- [1] M. Le Pallec, C. Kazmierski, E. Vergnol, S. Perrin, J.G. Provost, P. Dousière, G. Glastre, D. Carpentier, and S. Fabre, "New integrated buried laser-ridge modulator with identical active layer," *IEEE Photon. Technol. Lett.*, vol. 15, no. 3, pp. 362–365, Mar. 2003.
- [2] Jonathon S. Barton, Erik J. Skogen, Milan L. Masanovic, Steven P. DenBaars, and Larry A. Coldren, "Monolithic integration of Mach-Zehnder modulators with sampled grating distributed bragg reflector lasers," in *Technical Digest Integr. Photon. Res.* Jul. 17–19 2002, p. IFC3, Vancouver, Canada.
- [3] R.G. Broeke, J.J.M Binsma, M. van Geemert, F. Heinrichsdorff, T. van Dongen, J.H.C. van Zantvoort, X.J.M. Leijtens, Y.S. Oei, and M.K. Smit, "An all-optical wavelength converter with a monolithically integrated digitally tunable laser," in *Proc. 28th Eur. Conf. on Opt. Comm. (ECOC '02)*, Sept. 8–Sept. 12 2002, p. PD3.2, Copenhagen.
- [4] Wilfrid Pascher, Jan Hendrik den Besten, Davide Caprioli, Xaveer Leijtens, Meint Smit, and Raymond van Dijk, "Modelling and Design of a Travelling-Wave Electro-Optic Modulator on InP", *Opt. Quantum Electron.*, vol. 35, pp. 453–464, 2003, Special Issue on Optical Waveguide Theory and Numerical Modelling.
- [5] C.R. Doerr, M. Zirngibl, and C.H. Joyner, "Chirping of the waveguide grating router for free-spectral-range mode selection in the multifrequency laser," *IEEE Photon. Technol. Lett.*, vol. 8, no. 4, pp. 500–502, Apr. 1996.